Synthesis and Characterization of a Series of Monometallo-, Bimetallo-, and Heterobimetallo-1,2-Ethene-Linked Cofacial Bisporphyrins

Todd E. Clement, Daniel J. Nurco, and Kevin M. Smith*

Department of Chemistry, University of California, Davis, California 95616

Received June 23, 1997

The stepwise synthesis and characterization of a family of selectively metalated 1,2-bis[5-(2,3,7,8,12,13,17,18-octaethylporphyrinyl)]ethenes is described. These compounds are distinct from most of the previously reported bisporphyrin systems which possessed rigid linking groups or multiple strapping units, and their syntheses offer several advantages over the previously prepared systems. Among the members of this family we report the first heterobimetallic bisporphyrins able to exist as either cis (cofacial) or trans (extended) isomers including cis **13** {[Ni^{II}][Zn^{II}]}, cis **14** {[Ni^{II}][Cu^{II}]}, and trans **15** {[Cu^{II}][Mn^{III}]}. Products were characterized by ^{1}H NMR spectroscopy (except those containing Cu^{II} and/or Mn^{III}), visible spectroscopy, mass spectrometry, and elemental analyses. X-ray structural data are provided for bisporphyrins **4**, **10**, and **13**−**15**: cis **4** ($C_{74}H_{88}N_8Co_2$), monoclinic, space group $P2_1/c$, a = 21.097(15) Å, b = 14.120(5) Å, c = 22.987(11) Å, β = 108.59(4)°, Z = 4; cis **10** ($C_{74}H_{90}N_8Cu$) monoclinic, space group $P2_1/n$, a = 19.695(5) Å, b = 14.427(3) Å, c = 24.679(6) Å, β = 112.72-(2)°, Z = 4; cis **13** ($C_{74}H_{88}N_8NiZn$) monoclinic, space group $P2_1/c$, a = 21.187(3) Å, b = 13.9091(11) Å, c = 22.682(3) Å, β = 108.674(10)°, Z = 4; cis **14** ($C_{74}H_{88}N_8NiCu$) monoclinic, space group $P2_1/c$, a = 21.169(3) Å, b = 13.875(2) Å, c = 22.660(3) Å, β = 108.64(9)°, Z = 4; trans **15** ($C_{74}H_{88}N_8CuMnCl$), triclinic, space group $P\bar{1}$, a = 9.8123(13), b = 13.742(3), c = 14.774(3), α = 83.26(2), β = 78.532(12), γ = 78.347(14), Z = 1.

Introduction

Electron-transfer reactions play many important roles in nature. They are pivotal in photosynthesis and are a critical element in a diverse range of enzymatic processes. It is the importance and complexity of such biological functions that has led to the study of their chemistry in simplified model systems. The photosynthetic reaction center (PRC) proteins from *Rhodopseudomonas viridis* (*R.v.*) and *Rhodobacter spheroides* (*R.s.*) have been isolated in pure form and structurally characterized with X-ray crystallography.[1] These results have greatly aided efforts to model the early stages of photosynthesis. Of particular interest in the crystal structures of the PRCs are the "special pair" of bacteriochlorophyll monomers which are roughly coplanar and demonstrate a degree of macrocyclic overlap with a separation of approximately 3.6 Å. The model systems we present have been designed to closely mimic the spatial orientation observed in the special pair. In the present paper we demonstrate that *cis*-1,2-diporphyrinylethenes (**1**−**5**) (Chart 1) satisfy the above criteria, that the related *trans*-bisporphyrins (**6**−**8**) can also be obtained, and that it is possible to synthesize monometalated bisporphyrins (**9**−**12**) as well as heterobimetallic bisporphyrins in this series (**13**−**15**).

In the field of cofacial bisporphyrin chemistry most of the models developed thus far can be grouped into one of two classes: (1) compounds such as **16** and **17** (Chart 2), with two flexible strapping units linking the macrocycles;[2] (2) compounds (e.g. **18**−**20**) linked on one side of each macrocycle by a rigid[3] or flexible[4] linking unit. The syntheses of these types of compounds tend to be long and laborious, often requiring extensive chromatographic purifications[2a−c] and with relatively low yields of the target bisporphyrins. Bimetallic and heterobimetallic cofacial bisporphyrin systems have been shown to possess significant catalytic properties;[2a,3e,5] to date the bimetallic complexes which have shown the most promise are those of Co^{II} and Fe^{II}.[6] In addition, Mn^{II} complexes can function as oxygen coordinators and/or reducing agents.[7] Further, it is

(1) (a) Deisenhofer, J.; Epp, O.; Miki, K.; Huber, R.; Michel, H. *J. Mol. Biol.* **1984**, *180*, 385. (b) Deisenhofer, J.; Epp, O.; Miki, K.; Huber, R.; Michel, H. *Nature (London)* **1985**, *318*, 618. (c) Allen, J. P.; Feher, G.; Yeates, T. O.; Rees, D. C.; Deisenhofer, J.; Michel, H.; Huber, R. *Proc. Natl. Acad. Sci. U.S.A.* **1986**, *83*, 8589. (d) Allen, J. P.; Feher, G. *Proc. Natl. Acad. Sci. U.S.A.* **1984**, *81*, 4795. (e) Chang, C.-H.; Schiffer, M.; Tiede, D.; Smith, U.; Norris, J. *J. Mol. Biol.* **1985**, *186*, 201. (f) PDB coordinate file 1PSS; the crystal structure of the PRC from *Rhodobacter spheroides*: Chirino, A. J.; Lous, E. J.; Huber, M.; Allen, J. P.; Schenck, C. C.; Paddock, M. L.; Feher, G.; Rees, D. C. *Biochemistry* **1994**, *33*, 4584. (g) PDB coordinate file 1PRC; the PRC from *Rhodopseudomonas virdis*: Deisenhofer, J.; Epp, O.; Sinning, I.; Michel, H. *J. Mol. Biol.* **1995**, *246*, 429. (h) Abola, E. E.; Bernstein, F. C.; Bryant, S. H.; Koetzle, T. F.; Weng, J. Protein Data Bank. In *Crystallographic Databases*−*Information Content, Software Systems, Scientific Applications*; Allen, F. H., Bergerhoff, G., Sievers, R., Eds.; Data Commission of the International Union of Crystallography: Bonn, 1987; pp 107−132. Bernstein, F. C.; Koetzle, T. F.; Williams, G. J. B.; Meyer, E. F., Jr.; Brice, M. D.; Rodgers, J. R.; Kennard, O.; Shimanouchi, T.; Tasumi, M. The Protein Data Bank: A Computer-based Archival File for Macromolecular Structures. *J. Mol. Biol.* **1977**, *112*, 535.

(2) (a) Collman, J. P.; Denisevich, P.; Konai, Y.; Marroco, M.; Koval, C.; Anson, F. C. *J. Am. Chem. Soc.* **1980**, *102*, 6027. (b) Collman, J. P.; Anson, F. C.; Barnes, C. E.; Bencosme, C. S.; Geiger, T.; Evitt, E. R.; Kreh, R. P.; Meier, K.; Pettman, R. B. *J. Am. Chem. Soc.* **1983**, *105*, 2694. (c) Collman, J. P.; Elliott, C. M.; Halbert, T. R.; Tovrog, B. S. *Proc. Natl. Acad. Sci. U.S.A.* **1977**, *74*, 18. (d) Collman, J. P.; Bencosme, C. S.; Barnes, C. E.; Miller, B. D. *J. Am. Chem. Soc.* **1983**, *105*, 2704. (e) Collman, J. P.; Chong, A. O.; Jameson, G. B.; Oakley, R. T.; Rose, E.; Schmittou, E. R.; Ibers, J. A. *J. Am. Chem. Soc.* **1981**, *103*, 516. (f) Hatada, M.; Tulinsky, A., *Am. Crystallogr. Assoc. Ser. 2* **1980**, *8*, 34. (g) Hatada, M.; Tulinsky, A.; Chang, C. K., *J. Am. Chem. Soc.* **1980**, *102*, 7115. (h) Kimoon, K.; Collman, J. P.; Ibers, J. A. *J. Am. Chem. Soc.* **1988**, *110*, 4242. (i) Mamardashvili, N. Zh.; Zdanovich, S. A.; Tolubchikov, O. A. *Zh. Org. Khim.* **1996**, *32*, 934.

S0020-1669(97)00774-X CCC: $15.00
Published on Web 03/06/1998

Chart 1

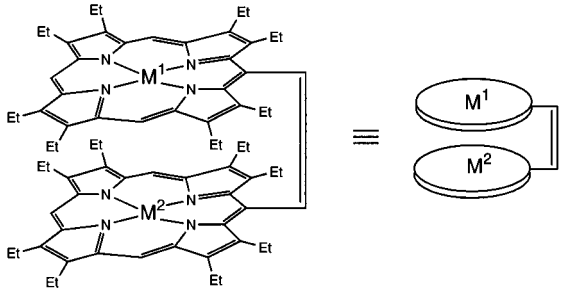

	1	2	3	4	5	9	10	13	14
M^1	2H	Ni(II)	Cu(II)	Co(II)	Fe(III)Cl	Ni(II)	Cu(II)	Ni(II)	Ni(II)
M^2	2H	Ni(II)	Cu(II)	Co(II)	Fe(III)Cl	2H	2H	Zn(II)	Cu(II)

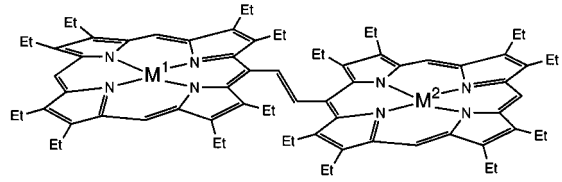

	6	7	8	11	12	15
M^1	2H	Ni(II)	Cu(II)	Zn(II)	Ni(II)	Cu(II)
M^2	2H	Ni(II)	Cu(II)	2H	2H	Mn(III)Cl

believed that a [Cu^{II}][Mn^{II}] cofacial bisporphyrin may be able to bind dioxygen at room temperature, without oxidation to a μ-oxo complex, and it is postulated that these two elements may have a donor−acceptor relationship through the cavity, quite possibly resulting in a good model for cytochrome *c* oxidase.[3h]

Chart 2

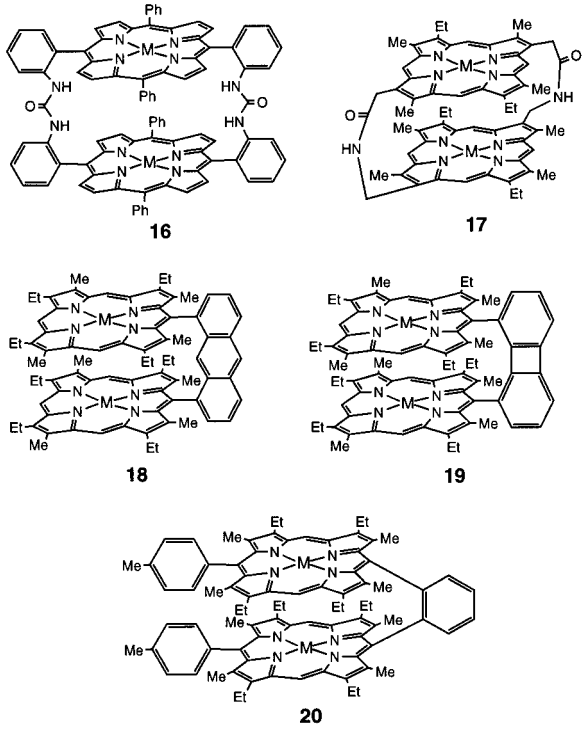

16 **17** **18** **19** **20**

Experimental Section

General Methods. Silica gel 60 (230−400 mesh) was used for flash chromatography; pressure was supplied by house compressed air. Solvents were purchased from Fisher and used as is for reactions, chromatography, and crystallization, except for 1,2-dimethoxyethane, which was distilled over $LiAlH_4$ prior to use in McMurry coupling reactions. ^{1}H NMR spectra were recorded on a Bruker QE 300 MHz instrument, and visible spectroscopy was performed using a Hewlett-Packard 8450A diode array spectrophotometer. Metal insertions, including workup and purification, were performed in the absence of light to ensure that photochemical isomerization of the bridging ethylenic bond, from cis to trans, did not occur.

Synthesis of Bimetallic and Heterobimetallic Bis(octaethylporphyrins). ***cis*-1,2-Bis[5-(2,3,7,8,12,13,17,18-octaethylporphyrinyl)]-ethene (1).** Free-base trans dimer **6** was converted into the cis isomer **1** utilizing the procedure of Ponomarev.[4d] A typical experiment is as follows: *trans*-Bisporphyrin **6** (444 mg, 0.406 mmol) was dissolved in acetic acid (400 mL), and the mixture was heated to reflux under an argon atmosphere for 40 min. The reaction vessel was then placed on a rotary evaporator and the volume reduced to ∼10 mL before neutralization with saturated Na_2CO_3. The aqueous layer was extracted with CH_2Cl_2 until clear and the organic layer subsequently washed with water (200 mL) and saturated NaCl (200 mL) prior to drying over Na_2SO_4 and filtering. Silica gel TLC (4% MeOH/CH_2Cl_2) of the reaction mixture after workup indicated an approximate ratio of 2:3 cis, **1**/trans **6**; flash chromatography on silica gel (3% MeOH/CH_2Cl_2 to collect **6**, 5% MeOH to elute **1**) allowed recovery of *trans*-bisporphyrin **6** and isolation of the desired product (**1**, 176 mg, 0.161 mmol, 40% conversion): vis [λ_{max} ($CHCl_3$)] 390 nm (ϵ 175 900), 474 (sh, 26 200), 528 (15 000), 594 (7200), 651 (2700); ^{1}H NMR ($CDCl_3$) δ −5.67, −4.84 (br s, 4H, NH), 0.75 (t, 12H), 1.49 (t, 24H), 1.88 (t, 12H), 2.55 (dq, 4H), 2.79 (dq, 4H), 3.33 (m, 8H), 3.62 (dq, 4H), 3.91 (dq, 4H), 4.13 (dq, 4H), 4.28 (dq, 4H), 8.03 (s, 4H, 10,20-H), 9.50 (s, 2H, 15-H), 9.69 (s, 2H, −C*H*═C*H*−). ^{1}H NMR as well as optical data matched those reported[4d] in the literature.

***trans*-1,2-Bis[5-(2,3,7,8,12,13,17,18-octaethylporphyrinyl)]-ethene (6).** The *trans*-octaethylporphyrin dimer (free base) was

(3) (a) Chang, C. K.; Abdalmuhdi, I. *J. Org. Chem.* **1983**, *48*, 5388. (b) Chang, C. K.; Abdalmuhdi, I. *Angew. Chem., Int. Ed. Engl.* **1984**, *23*, 164. (c) Guilard, R.; Lopez, M. A.; Tabard, A.; Richard, P.; Lecomte, C.; Brandès, S.; Hutchison, J. E.; Collman, J. P. *J. Am. Chem. Soc.* **1992**, *114*, 9877. (d) Osuka, A.; Nakajima, S.; Nagata, T.; Maruyama, K.; Toriumi, K. *Angew. Chem., Int. Ed. Engl.* **1991**, *30*, 582. (e) Collman, J. P.; Hutchinson, J. E.; Lopez, M. A.; Tabard, A.; Guilard, R.; Soek, W. K.; Ibers, J. A.; L'Her, M. *J. Am. Chem. Soc.* **1992**, *114*, 9869. (f) Sessler, J. L.; Johnson, M. R.; Creager, S. E.; Fettinger, J. C.; Ibers, J. A. *J. Am. Chem. Soc.* **1990**, *112*, 9310. (g) Naruta, Y.; Sawada, N.; Tadokoro, M. *Chem. Lett.* **1994**, 1713. (h) Guilard, R.; Brandes, S.; Tabard, A.; Bouhmaida, N.; Lecomte, C.; Richard, P.; Latour, J.-M. *J. Am. Chem. Soc.* **1994**, *116*, 10202. (i) Fillers, J. P.; Ravichandran, K. G.; Abdulmuhdi, I.; Tulinsky, A.; Chang, C. K. *J. Am. Chem. Soc.* **1986**, *108*, 417.

(4) (a) Senge, M. O.; Gerzevske, K. R.; Vicente, M. G. H.; Forsyth, T. P.; Smith, K. M. *Angew. Chem., Int. Ed. Engl.* **1993**, *32*, 750. (b) Senge, M. O.; Gerzevske, K. R.; Vicente, M. G. H.; Forsyth, T. P.; Smith, K. M. *Inorg. Chem.* **1994**, *33*, 5625. (c) Landrum, J. T., Grimett, D., Haller, K. J., Scheidt, W. R.; Reed, C. A. *J. Am. Chem. Soc.* **1981**, *103*, 2640. (d) Ponomarev, G. V.; Borovkov, V. V.; Sugiura, K.; Yoshiteru, S.; Shul'ga, A. M. *Tetrahedron. Lett.* **1993**, *34*, 2153. (e) Clezy, P. S.; Craig, D. C.; James, V. J.; McConnell, J. F.; Rae, A. D. *Acta Crystallogr., Sect. C* **1979**, *8*, 605.

(5) (a) Collman, J. P.; Wagenknecht, P. S.; Lewis, N. S. *J. Am. Chem. Soc.* **1992**, *114*, 5665. (b) Collman, J. P.; Hutchinson, J. E.; Lopez, M. A.; Guilard, R. *J. Am. Chem. Soc.* **1992**, *114*, 8066. (c) Sessler, J. L.; Johnson, M. R.; Creager, S. E.; Fettinger, J. C.; Ibers, J. A. *J. Am. Chem. Soc.* **1990**, *112*, 9310. (d) Collman, J. P.; Tyvoll, D. A.; Chang, L.; Fish, H. T. *J. Org. Chem.* **1995**, *60*, 1926. (e) Collman, J. P.; Wagenknecht, P. S.; Hutchinson, J. E. *Angew. Chem., Int. Ed. Engl.* **1994**, *33*, 3, 1537. (f) Naruta, Y.; Sasayama, M.; Sasaki, T. *Angew. Chem., Int. Ed. Engl.* **1994**, *33*, 3, 1839.

(6) (a) Basolo, F.; Hoffman, B. M.; Ibers, J. A. *Acc. Chem. Res.* **1975**, *8*, 384. (b) Durand, R. R., Jr.; Bencosme, C. S.; Collman, J. P.; Anson, F. C. *J. Am. Chem. Soc.* **1983**, *105*, 2710. (c) Guilard, R.; Brandes, S.; Tardieux, C.; Tabard, A.; L'Her, M.; Miry, C.; Gouerec, P.; Knop, Y.; Collman, J. P. *J. Am. Chem. Soc.* **1995**, *117*, 11721.

(7) (a) Jones, D. R.; Summerville, D. A.; Basolo, F. *Chem. Rev.* **1979**, *79*, 139. (b) Naruta, Y.; Maruyama, K. *J. Am. Chem. Soc.* **1991**, *113*, 3595.

prepared in 56% yield via McMurry coupling of the copper complex of 5-formyloctaethylporphyrin,[4b] followed by demetalation with 15% H_2SO_4/TFA.

***cis*-1-[Nickel(II) 5-(2,3,7,8,12,13,17,18-octaethylporphyrinyl)]-2-[5-(2,3,7,8,12,13,17,18-octaethylporphyrinyl)]ethene (9).** Compound **1** (175 mg, 0.16 mmol) was added to a dilute solution of $Ni(OAc)_2$ (39.7 mg, 0.16 mmol) in DMF (455 mL). The reaction mixture was heated to 105−110 °C for 2 h, after which spectrophotometry and silica gel TLC indicated the major chromophore to be the monometalated species. The mixture was then poured into ice−water and extracted with CH_2Cl_2. The CH_2Cl_2 layer was washed with water (2 × 100 mL) and brine (100 mL) and dried over Na_2SO_4. The solvent was evaporated, and the crude product was purified by column chromatography on silica gel. The least polar fraction (red) eluted with CH_2Cl_2 and was identified as the dimetalated product. The middle fraction was collected with 1% MeOH/CH_2Cl_2 as eluent and yielded the title compound **9** (76 mg, 0.066 mmol) in 41% yield. The remainder of the starting material eluted with 3% MeOH/CH_2Cl_2: mp (dec) 259−263 °C; vis [λ_{max} (CH_2Cl_2)] 392 nm (ϵ 181 900), 524 (12 400), 546 (11 300), 588 (11 100); ^{1}H NMR ($CDCl_3$) δ −5.64 (br s, 1H), −4.75 (br s, 1H), 0.72 (t, 6H), 0.87 (t, 6H), 1.19 (t, 6H), 1.32 (t, 6H), 1.68 (m, 18H), 1.95 (t, 6H), 2.68 (m, 4H), 2.83 (m, 8H), 2.99 (m, 4H), 3.29 (m, 2H), 3.62 (m, 2H), 3.86 (m, 4H), 4.05 (m, 4H), 4.23 (m, 4H), 7.77 (s, 2H), 8.53 (s, 2H), 9.01 (s, 1H), 9.34 (d, 1H, J = 11 Hz), 9.53 (d, 1H, J = 11 Hz), 9.68 (s, 1H). Anal. Calcd for $C_{74}H_{90}N_8Ni\cdot H_2O$: C, 76.08; H, 7.94; N, 9.59. Found: C, 76.41; H, 7.59; N, 9.63. MS [*m*/*z* (rel intensity %)]: 1150 (M^+, 100).

***cis*-1-[Copper(II) 5-(2,3,7,8,12,13,17,18-octaethylporphyrinyl)]-2-[5-(2,3,7,8,12,13,17,18-octaethylporphyrinyl)]ethene (10).** Bisporphyrin **1** (230 mg, 0.21 mmol) was added to a dilute solution of $Cu(OAc)_2$ (50 mg, 0.20 mmol) in DMF (575 mL). The mixture was heated to 105−110 °C for 35 min, at which time spectrophotometry and TLC showed the monometalated species to be the major product. The workup and purification were identical with that given for compound **9**. The monometalated bisporphyrin **10** (126 mg, 0.11 mmol) was obtained in 55% yield after chromatography: mp (dec) 261−265 °C; vis [λ_{max} (CH_2Cl_2)] 392 nm (ϵ 201 000), 548 (11 300), 588 (10 200). Anal. Calcd for $C_{74}H_{90}CuN_8\cdot 3H_2O$: C, 73.51; H, 8.00; N, 9.27. Found: C, 73.44; H, 7.69; N, 9.31. MS [*m*/*z* (rel intensity %)]: 1155 (M^+, 100).

***cis*-1-[Nickel(II) 5-(2,3,7,8,12,13,17,18-octaethylporphyrinyl)]-2-[zinc(II) 5-(2,3,7,8,12,13,17,18-octaethylporphyrinyl)]ethene (13).** Compound **9** (100 mg, 0.087 mmol) was added to a solution of $Zn(OAc)_2$ (320 mg, 1.46 mmol) in MeOH (30 mL), and CH_2Cl_2 (30 mL) and the mixture was brought to reflux. The reaction was shown to be complete by spectrophotometry after 1 h at reflux. After aqueous workup and evaporation of the solvent, column chromatography on silica gel with 50% petroleum ether/CH_2Cl_2 as eluent, followed by crystallization from CH_2Cl_2/MeOH, gave the title compound (81 mg, 0.067 mmol) in 76% yield: mp >300 °C; vis [λ_{max} (CH_2Cl_2)] 392 nm (ϵ 229 000), 562 (21 300); ^{1}H NMR ($CDCl_3$) δ 1.06 (t, 6H, J = 7.5 Hz), 1.13 (t, 6H, J = 7.5 Hz), 1.31 (t, 6H, J = 7.5 Hz), 1.36 (t, 6H, J = 7.5 Hz), 1.71 (m, 18H, J = 7.5 Hz), 1.95 (t, 6H, J = 7.5 Hz), 3.12 (m, 8H), 3.21 (m, 4H), 3.33 (m, 2H), 3.45 (m, 2H), 3.65 (m, 2H), 3.91 (m, 6H), 4.11 (m, 2H), 4.36 (m, 6H), 7.76 (s, 2H), 8.54 (s, 1H), 8.57 (s, 2H), 9.46 (d, 1H, J = 11 Hz), 9.52 (d, 1H, J = 11 Hz), 9.74 (s, 1H). Anal. Calcd for $C_{74}H_{88}N_8NiZn\cdot 2H_2O$: C, 71.12; H, 7.42; N, 8.97. Found: C, 71.52; H, 7.16; N, 8.97. MS [*m*/*z* (rel intensity %)]: 1213 (M^+, 100).

***cis*-1-[Nickel(II) 5-(2,3,7,8,12,13,17,18-octaethylporphyrinyl)]-2-[copper(II) 5-(2,3,7,8,12,13,17,18-octaethylporphyrinyl)]ethene (14).** This bisporphyrin was prepared using $Cu(OAc)_2$ (excess) in MeOH/CH_2Cl_2 with the procedure described for compound **13** and was obtained in 65% yield after purification: mp (dec) 275−278 °C; vis [λ_{max} (CH_2Cl_2)] 394 nm (ϵ 228 000), 572 (20 700). Anal. Calcd for $C_{74}H_{88}CuN_8Ni$: C, 73.35; H, 7.32; N, 9.25. Found: C, 73.29; H, 7.42; N, 9.29. MS [*m*/*z* (rel intensity %)]: 1212 (M^+, 100).

***trans*-1-[Chloromanganese(III) 5-(2,3,7,8,12,13,17,18-octaethylporphyrinyl)]-2-[copper(II) 5-(2,3,7,8,12,13,17,18-octaethylporphyrinyl)]ethene (15).** DMF (62 mL) was added to bisporphyrin **10** (120 mg, 0.104 mmol) and $MnCl_2$ (107 mg, 0.54 mmol), and the mixture was heated to reflux while stirring for 2 h. After this time, an additional portion of $MnCl_2$ (100 mg, 0.51 mmol) was added and reflux was continued for another 2 h. Spectrophotometric (absorbance maximum at 478 nm characteristic of manganese porphyrins) and chromatographic analysis after 4 h of reflux indicated that the manganese insertion was complete. The reaction workup was the same as for compounds **9** and **10**, and purification by column chromatography using silica gel, eluted with 5% MeOH/CH_2Cl_2, yielded the *trans*-bisporphyrin **15**. Crystallization from CH_2Cl_2/*n*-hexane gave bisporphyrin **15** (56 mg, 0.045 mmol) in 47% yield: mp (dec) 247−250 °C; vis [λ_{max} (CH_2Cl_2)] 408 nm (ϵ 253 000), 478 (69 500), 534 (22 400), 570 (24 800). Anal. Calcd for $C_{74}H_{88}ClCuMnN_8$: C, 71.52; H, 7.14; N, 9.02. Found: C, 71.20; H, 7.26; N, 9.26. MS [*m*/*z* (rel intensity %)]: 1213 (M^+ − Cl, 100).

***cis*-1,2-Bis[cobalt(II) 5-(2,3,7,8,12,13,17,18-octaethylporphyrinyl)]-ethene (4).** Compound **1** (57 mg, 0.052 mmol) was added to CH_2Cl_2 (20 mL, distilled over CaH_2), and the mixture was brought to reflux under an argon atmosphere before 1 mL of a saturated solution of $Co(OAc)_2$ in MeOH was added to the reaction flask via syringe. The mixture was heated at reflux for 1.5 h, after which time spectrophotometry indicated the metal insertion to be complete. Upon aqueous workup and removal of the solvent, crystallization from CH_2Cl_2/MeOH yielded the title compound (45 mg, 0.037 mmol) in 72% yield: mp (dec) 272−275 °C; vis [λ_{max} (CH_2Cl_2)] 387 nm (ϵ 184 800), 566 (14 300); ^{1}H NMR ($CDCl_3$) δ 2.58 (br s, 12H), 4.52 (br s, 16H), 4.83 (br s, 16H), 5.97 (br s, 4H), 6.42 (br s, 12H), 8.65 (br s, 4H), 8.96 (br s, 4H), 9.23 (br s, 4H), 12.46 (br s, 4H), 12.79 (br s, 4H), 16.48 (br s, 4H), 19.52 (br s, 2H), 29.02 (br s, 2H). Anal. Calcd for $C_{74}H_{88}Co_2N_8$: C, 73.60; H, 7.35; N, 9.28. Found: C, 73.21; H, 7.42; N, 9.33. MS [*m*/*z* (rel intensity %)]: 1207 (M^+, 100).

***cis*-1,2-Bis[Chloroiron(III) 5-(2,3,7,8,12,13,17,18-octaethylporphyrinyl)]ethene (5).** This bisporphyrin was prepared using standard methodology[8] from compound **1** as follows. Bisporphyrin **1** (60 mg, 0.055 mmol) was dissolved in $CHCl_3$ (12 mL, degassed) and added via dropping funnel to a mixture of $FeCl_2$ (300 mg, 1.51 mmol) and CH_3CN (25 mL, refluxed under argon for 1 h prior to addition of $FeCl_2$) at 50 °C. The reaction mixture was stirred for 35 min at 50 °C under argon and then exposed to air and stirred for an additional 30 min at room temperature. The mixture was washed with 2 N HCl (1 × 125 mL) followed by the normal aqueous workup and evaporation of the solvent. Crystallization from CH_2Cl_2/*n*-hexane gave the desired product (46 mg, 0.036 mmol) in 67% yield: mp (dec) 265−270 °C; vis [λ_{max} (CH_2Cl_2)] 390 nm (ϵ 123 200), 510 (14 300), 646 (5500); ^{1}H NMR (FeCN complex, CD_3OD) δ −9.96 (br s, 4H), −7.48 (br s, 2H), 2.24 (br s, 24H), 2.41 (br s, 12H), 2.64 (br s, 12H), 4.04 (br s, 4H), 4.78 (br s, 4H, coincident with solvent peak), 5.99 (br s, 4H), 6.38 (br s, 10H), 6.94 (br s, 4H), 8.75 (br s, 4H), 14.70 (br s, 4H). MS [*m*/*z* (rel intensity %)]: 1270 (M^+, 16), 1235 (M^+ − Cl, 80), 1200 (M^+ − 2Cl, 99).

X-ray Crystallographic Experimental Data. A dark purple prismatic crystal of **4** with dimensions 0.70 × 0.50 × 0.38 mm was grown from MeOH/CH_2Cl_2. A dark purple parallelepiped crystal of **10** with dimensions 0.80 × 0.60 × 0.40 mm was grown from MeOH/benzene. A purple prismatic crystal of **13** with dimensions 0.64 × 0.36 × 0.30 mm was grown from MeOH/CH_2Cl_2. A brick red prismatic crystal of **14** with dimensions 0.80 × 0.80 × 0.40 mm was grown from MeOH/CH_2Cl_2. A dark purple triangular crystal of **15** with dimensions 0.20 × 0.16 × 0.06 mm was grown from cyclohexane/CH_2Cl_2. The crystals of **10** and **13**−**15** were transferred directly from their mother liquors of crystallization to a light hydrocarbon oil (Paratone N) in which they were examined under a microscope and suitable specimens were selected. A Siemens P4 diffractometer equipped with a modified Siemens LT-2 cooling device and a rotating anode [λ(Cu Kα) = 1.541 78 Å (nickel filtered)] operating at 15.0 kW was used for **13** and **15**. A Syntex $P2_1$ diffractometer equipped with a modified Siemens LT-1 cooling device and a normal-focus sealed tube [λ(Cu Kα) = 1.541 78 Å (graphite monochromated)] operating at 2.0 kW was used for **10** and **14**. The crystal selected for **4** was allowed to dry after removal from its mother liquor of crystallization and was subsequently affixed to a glass fiber with a small amount of

(8) Langry, K. C. Ph.D. Dissertation, University of California, Davis, 1982; p 325.

Table 1. Crystallographic Data for Compounds **4**, **10**, and **13**−**15**

	4	**10**	**13**	**14**	**15**
chem formula	$C_{74}H_{88}N_8Co_2$	$C_{74}H_{90}N_8Cu$	$C_{74}H_{88}N_8NiZn$	$C_{74}H_{88}N_8NiCu$	$C_{74}H_{88}N_8CuMnCl$
fw	1207.45	1155.44	1213.65	1211.83	1243.52
space group	$P2_1/c$ (No. 14)	$P2_1/n$ (No. 14)	$P2_1/c$ (No. 14)	$P2_1/c$ (No. 14)	$P\bar{1}$ (No. 2)
a (Å)	21.10(2)	19.695(5)	21.187(3)	21.169(3)	9.8123(13)
b (Å)	14.120(5)	14.427(3)	13.9091(11)	13.875(2)	13.742(3)
c (Å)	22.987(11)	24.679(6)	22.682(3)	22.660(3)	14.774(3)
α (deg)	90	90	90	90	83.26(2)
β (deg)	108.59(4)	112.72(2)	108.674 (10)	108.64(9)	78.532(12)
γ (deg)	90	90	90	90	78.347(14)
V (Å^3)	6490(6)	6468(3)	6332.1(13)	6306.43(14)	1905.9(7)
Z	4	4	4	4	1
T (K)	293(2)	130(2)	130(2)	130(2)	130(2)
λ (Å)	0.710 73	1.541 78	1.541 78	1.541 78	1.541 78
ρ_{calcd} (g cm^{-3})	1.236	1.184	1.267	1.277	1.144
2θ(min/max) (deg)	3.44/45.00	4.92/113.8	4.40/112.38	4.40/114.16	6.12/112.12
scan type	ω	$\theta-2\theta$	$\theta-2\theta$	$\theta-2\theta$	$\theta-2\theta$
octants collcd	$+h,+k,\pm l$	$+h,+k,\pm l$	$+h,+k,\pm l$	$+h,+k,\pm l$	$+h,\pm k,\pm l$
tot. reflcns	9177	9402	8942	9203	5937
unique reflcns	9177	8681	8269	8508	4977
R_{int}		0.036	0.033	0.066	0.039
obsd reflcns	5943 ($>2\sigma(I)$)	7546 ($>2\sigma(I)$)	7546 ($>2\sigma(I)$)	7738 ($>2\sigma(I)$)	4027 ($>2\sigma(I)$)
μ (mm^{-1})	0.56	0.839	1.209	1.163	2.684
min/max transm	0.79/0.84	0.68/0.75	0.69/0.74	0.46/0.67	0.65/0.86
$R(F_o^2)$ ($>2\sigma(I)$)[a]	0.060	0.048	0.051	0.047	
$R_w(F_o^2)$ (all data)[a]	0.1860	0.124	0.175	0.124	

[a] $R1 = \Sigma||F_o - F_c||/\Sigma|F_o|$ and $wR2 = [\Sigma[w(F_o^2 - F_c^2)^2]/\Sigma[w(F_o^2)^2]]^{1/2}$. [b] $w = 1/[\sigma^2(F_o^2) + ((X)P)^2 + (Y)P]$, where $P = (F_o^2 + 2F_c^2)/3$. For **10**, $X = 0.0528$ and $Y = 7.0826$, for **13**, $X = 0.0949$ and $Y = 17.5189$, for **14**, $X = 0.0601$ and $Y = 9.7021$, and, for **4**, $X = 0.0880$ and $Y = 5.2298$.

polyester resin. The crystal was then mounted on a Siemens R3m/V diffractometer equipped with a normal-focus sealed tube source [λ(Mo Kα) = 0.710 73 Å (graphite monochromated)] operating at 2.0 kW for cell determination and data collection at room temperature.

The Siemens SHELXTL V. 5.03 software package was used for structure solution and refinement. Structures were solved via direct methods and refined (based on F^2 using all independent data) by full-matrix least-squares methods. Empirical absorption corrections were applied to the datasets.[9] Unless otherwise noted, all non-hydrogen atoms were refined with anisotropic thermal parameters. Hydrogens were generated by their idealized geometry and treated as riding using fixed isotropic thermal parameters related to the thermal parameter of the adjacent bonded carbon atom. The structure of **10** exhibited inversion of the porphyrin macrocycles in a ratio of 85/15 as evidenced by the relative occupancies of Cu^{II} in the center of each macrocycle. Additionally in the structure of **10** there was disorder in the positions of 2 Cβ's and their attached ethyl groups. Each disordered atom was refined with 2 sites; relative occupancies for each pair of disordered sites were allowed to refine freely but with the restriction that the total occupancy was 100% for each atom. The disordered atoms in the structure of **10** were refined with isotropic thermal parameters. The asymmetric unit of **15** was one porphyrin macrocycle possessing 2 metal sites and a 0.50 axial chloride indicating a statistical disorder among the Cu^{II}- and Mn^{III}-containing macrocycles. Crystallographic mention of **15** is made herein in order to confirm the trans configuration of the bisporphyrin-linking ethylenic bond; full structural details for **15** are not presented. Further details regarding the experimental data for the crystal structures described above are presented in Table 1. Crystallographic information files for **4**, **10**, **13**, and **14** have been deposited with the Cambridge Crystallographic Data Centre for inclusion in the Cambridge Structural Database.

Results and Discussion

The most successful cofacial bisporphyrin systems studied to date appear to be related to the so-called "Pac-Man" porphyrin systems (e.g. **18**−**20**).[3e,h,6c,10] As mentioned previously, though synthetic routes to Pac-Man systems have been improved,[3c,e] these fairly rigid coplanar bisporphyrins still pose a formidable challenge for synthetic chemists. However, the ligand system we have focused on can be prepared in moderate yields in two steps from the Cu^{II} complex of octaethylporphyrin. Furthermore, cofacial (cis: e.g. **1**−**5**, **9**, **10**, **13**, **14**) as well as extended (trans: e.g. **6**−**8**, **11**, **12**,[11] **15**) isomers can be prepared, both of which may be helpful in studying physical, catalytic, and other chemical phenomena. Four of the bimetallic bisporphyrins, (**2**, **3**, **7**, and **8**) have been reported elsewhere.[4a,b] The 1,2-ethene system **1** possesses a great deal of flexibility, both horizontally and vertically, compared with the Pac-Man porphyrins. In addition to being a potential model for the photosynthetic special pair, this ligand might also serve as a model for electron-transfer systems (via selective metalation of the two porphyrin rings so as to provide a redox gradient between the two π-interacting components) or as a catalyst (by binding of certain ligands between the two porphyrin faces of this dynamically flexible system). Finally, definitive assessment of the extent of intra- versus intermolecular phenomena can be determined by use of the extended (trans) compounds derived from **6** for comparison purposes.

Heterobimetallic Bisporphyrins. The metal-free cofacial bisporphyrin **1** was prepared from the trans isomer **6** using the procedure of Ponomarev.[4d] The trans isomer **6** was prepared in 56% yield via McMurry coupling of the Cu^{II} complex of 5-formyloctaethylporphyrin,[4b] followed by demetalation with 15% H_2SO_4/TFA. To synthesize the heterobimetallic species **13** and **14**, we needed to initially selectively metalate one of the porphyrin macrocycles in **1** while maintaining the other macrocycle as a free base. In recent years, Sessler synthesized monozinc bisporphyrins by using 1.3 equiv of $Zn(OAc)_2$.[5c] This can also be accomplished by using an excess of the metalating reagent [$M(OAc)_2$] and monitoring the reaction by TLC and spectrophotometry, which tends to produce predominately dimetalated products, or by using only 1 equiv of $M(OAc)_2$ under dilute conditions (DMF, 108 °C) to potentially give the

(9) Parkin, S. R.; Moezzi, B.; Hope, H. *J. Appl. Crystallogr.* **1995**, *28*, 53.

Scheme 1

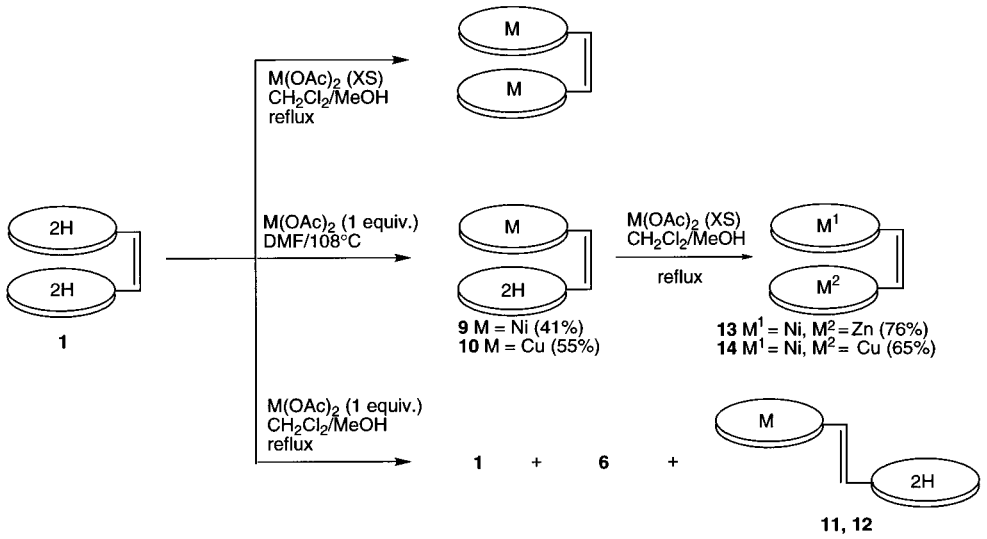

monometalated species (compounds **9** and **10**) as the major product (Scheme 1).

Initially, metal insertion into **1** was attempted using 1 equiv of $M(OAc)_2$ in CH_2Cl_2/MeOH (dilute conditions, at reflux); however, the majority of the starting material had isomerized to the less sterically hindered trans conformer **6** before metal insertion took place (Scheme 1). For example, when attempts were made to prepare the cis monozinc(II) derivative, the product obtained was shown (λ_{max} 406, 424 nm) to be the trans compound **11**. It appears that isomerization takes place photochemically and/or when the cis di-free base or monometalated species are left in solution for extended periods. To slow the isomerization the rate of metal insertion had to be increased; this was accomplished by utilizing a higher boiling solvent (DMF, Scheme 1). Monometalation of **1** via this method afforded the desired cofacial monometallo-bisporphyrins **9** and **10**. The ^{1}H NMR spectrum of mononickel bisporphyrin **9** was particularly diagnostic regarding a number of structural issues. The cis configuration of the linking ethylenic bond was confirmed by the presence of two doublets which displayed a coupling constant characteristic of cis-substituted ethenes ([$-CH^1{=}CH^2-$]: H^1 δ 9.34, doublet, 1H, J = 11 Hz; H^2 δ 9.53, doublet, 1H, J = 11 Hz). Nonequivalence of the two porphyrin macrocycles was established by the presence of four C_{meso} signals (δ 7.77, singlet, 2H; δ 8.53, singlet 2H; δ 9.01, singlet, 1H; δ 9.68, singlet, 1H). Finally, the identification of one macrocycle as a metalloporphyrin was established by the lack of NH signals for that macrocycle, and the free-base character of the second macrocycle was confirmed by the presence of 2 NH signals (δ -5.64, singlet, 1H; δ -4.75, singlet, 1H). In the case of monocopper bisporphyrin **10**, confirmation of the cis configuration of the linking ethylenic bond and the presence of a Cu^{II} ion in one macrocycle and the lack thereof in the other was facilitated by an X-ray crystallographic analysis (Figure 1).

Metal insertion to form the heterobimetallic compounds **13** and **14** was accomplished by the use of an excess of $M(OAc)_2$ (Scheme 1) since over-metalation (and transmetalation) was no longer a concern. The heterobimetallic cofacial bisporphyrins **13** and **14** were obtained after chromatography and crystallization, in 76 and 65% yields, respectively. Unlike the cis di-free base and monometallo bisporphyrins in this series, the bimetallic and heterobimetallic bisporphyrins demonstrated a greater stability toward photochemical and/or solution-state isomerization of their linking ethylenic bonds. X-ray crystal structures for both **13** and **14** (Figures 2 and 3, respectively) confirmed that these bisporphyrins maintained cofacial conformations. In addition, examination of the ^{1}H NMR spectrum of the diamagnetic bisporphyrin **13** confirmed, as in the case of **9**, that the conformation of the linking ethylenic bond was cis ([$-CH^1{=}CH^2-$]: H^1 δ 9.46, doublet, 1H, J = 11 Hz; H^2 δ 9.52, doublet, 1H, J = 11 Hz), that the two porphyrin rings were nonequivalent (four C_{meso} signals: δ 7.76, singlet, 2H; δ

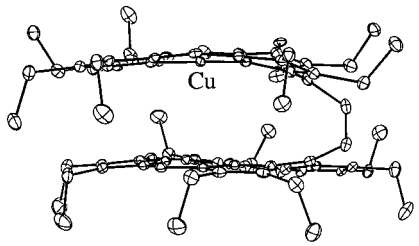

Figure 1. Molecular structure of bisporphyrin **10** illustrated with 35% probability thermal ellipsoids. Hydrogens have been omitted for clarity.

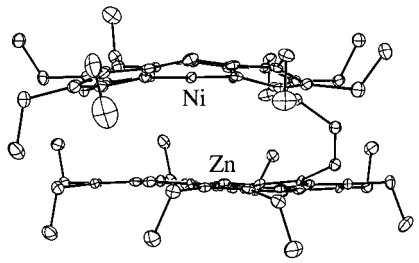

Figure 2. Molecular structure of bisporphyrin **13** illustrated with 35% probability thermal ellipsoids. Hydrogens have been omitted for clarity.

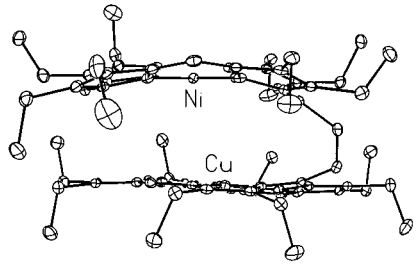

Figure 3. Molecular structure of bisporphyrin **14** illustrated with 35% probability thermal ellipsoids. Hydrogens have been omitted for clarity.

Scheme 2

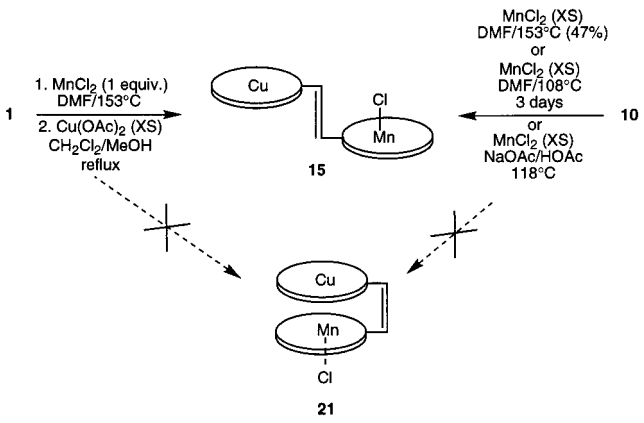

8.54, singlet, 1H; δ 8.57, singlet, 2H; δ 9.74, singlet, 1H), and that both macrocycles were metalated (due to the lack of NH signals).

Due to our success in the synthesis of heterobimetallic bisporphyrins **13** and **14**, we decided to investigate the synthesis and properties of the [Cu^{II}][Mn^{III}] bisporphyrin **21** in order to make comparisons with the more rigid biphenylene linked [Cu^{II}]-[Mn^{III}] bisporphyrin **19** prepared by Guilard and co-workers.[3h] To prepare **21**, bisporphyrin **10** was treated with an excess of $MnCl_2$ in DMF[12] and heated until spectrophotometry indicated manganese insertion was complete (Scheme 2). Column chromatography (silica gel) and crystallization yielded a product that was clearly a [Cu^{II}][Mn^{III}] bisporphyrin (elemental analysis; LRMS), but X-ray crystallography revealed that the product was the trans isomer **15** and not the desired cis isomer **21**. The structure of the starting material for this reaction (**10**) had been definitively shown to possess the cis-configuration, and hence, we concluded that isomerization of the bridging double bond occurred under the elevated temperatures used for manganese insertion. Attempts were therefore made, using other approaches, to synthesize the cofacial compound **21** (Scheme 2). Additional manganese insertions using bisporphyrin **10** as the starting material were attempted; one followed the procedure described above, but at 108 °C for 3 days, and another followed the procedure described by Fuhrhop and Smith.[13] Both reactions produced the undesired trans-product (**15**). When bisporphyrin **1** was used as the starting material and manganese was inserted first, followed by insertion of copper, **15** was again the only product.

To determine if the isomerization that occurred during manganese insertion was a one-time isomerization related to the reaction, and if the cis isomer **21** could be obtained from the trans mono-Cu^{II} compound, a synthesis was undertaken starting with the extended isomer **6**. When **6** was subjected to the monometalation conditions used to prepare **10**, it was discovered that metal insertion was much faster and more selective than in the case of the **10** resulting in trans di-Cu^{II} **8** as the major product, along with a significant recovery of starting material and very little of the desired trans mono-Cu^{II} compound. The dimetalated complex was the major product, independent of whether Cu^{II} or Mn^{III} was inserted first. We have concluded that the free-base macrocycle becomes activated (or less deactivated) toward metal insertion once monometalation has occurred. This was discovered to be the case even when less than 1 equiv of $M(OAc)_2$ was used. When the monocopper trans bisporphyrin was obtained, as a mixture with the dicopper complex, separation was virtually impossible due to the insolubility of both complexes. However, after the mixture was subjected to Mn^{III} insertion conditions, the product **15** was more soluble than the di-Cu^{II} byproduct **8** of the monometalation reaction, and thus a separation was possible via solubilizing **15** followed by filtration. Unfortunately, isomerization of the trans mono-Cu^{II} compound did not accompany Mn^{III} insertion, and the product obtained was merely the trans isomer **15** (determined by spectrophotometry).

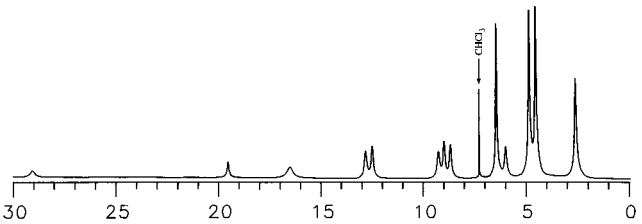

Figure 4. ^1H NMR spectrum of the di-Co^{II} porphyrin **4** in $CDCl_3$.

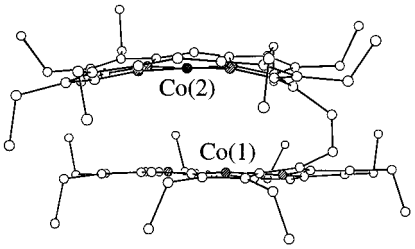

Figure 5. Molecular structure of bisporphyrin **4**. Hydrogens have been omitted for clarity.

Bimetallic Cofacial Bisporphyrins. The di-Co^{II} cofacial bisporphyrin **4** was synthesized according to the procedure described by Medforth et al.[14] The visible absorption spectrum of the product was clearly that of a metalloporphyrin, and the ^1H NMR spectrum (Figure 4) displayed the characteristic paramagnetic shifts and peak broadening expected of a low-spin Co^{II} porphyrin complex.[14] In addition, it was apparent from the ^1H NMR spectrum that the bisporphyrin was in the cofacial orientation (cis), as evidenced by the presence of eight diastereotopic methylene proton signals. The molecular structure of compound **4** was further established by X-ray crystallography (Figure 5).

The di-Fe^{III} cofacial bisporphyrin **5** was prepared following the metalation procedure of Langry,[8] to afford a product with a visible spectrum characteristic of an Fe^{III} porphyrin. To obtain more structural information, the low-spin Fe^{III} cyanide complex of compound **5** was analyzed by ^1H NMR spectroscopy; the spectrum (Figure 6) displayed paramagnetic shifts and resonances typical of low-spin Fe^{III} cyanide.[15] Of interest were multiple resonances for the diastereotopic methylene protons, once again confirming the cofacial orientation of compound **5**.

(10) (a) Collman, J. P.; Hutchison, J. E.; Wagenknecht, P. S.; Lewis, N. S.; Lopez, M. A.; Guilard, R. *J. Am. Chem. Soc.* **1990**, *112*, 8206. (b) Collman, J. P.; Hutchison, J. E.; Lopez, M. A.; Guilard, R.; Reed, R. A. *J. Am. Chem. Soc.* **1991**, *113*, 2794. (c) Collman, J. P.; Hutchison, J. E.; Lopez, M. A.; Guilard, R. *J. Am. Chem. Soc.* **1992**, *114*, 8066. (d) Collman, J. P.; Hutchison, J. E.; Ennis, M. S.; Lopez, M. A.; Guilard, R. *J. Am. Chem. Soc.* **1992**, *114*, 8074.

(11) Yashunskii, D. V.; Ponomarev, G. V.; Arnold, D. P. *Khim. Geterotsikl. Soedin.* **1996**, 1659.

(12) Adler, A. D.; Longo, F. R.; Kampas, F.; Kim, J. *J. Inorg. Nucl. Chem.* **1970**, *32*, 2443.

(13) Fuhrhop, J.-H.; Smith, K. M. In *Porphyrins and Metalloporphyrins*, Smith, K. M., Ed.; Elsevier: Amsterdam, 1975; p 797.

(14) Medforth, C. J.; Hobbs, J. D.; Rodriquez, M. R.; Abraham, R. J.; Smith, K. M.; Shelnutt, J. A. *Inorg. Chem.* **1995**, *34*, 1333.

(15) Scheidt, W. R.; Haller, K. J.; Hatano, K. *J. Am. Chem. Soc.* **1980**, *102*, 3017.

Table 2. Crystallographically Derived Intradimer Geometrical Features for Compounds **2**−**4**, **10**, **13**, and **14** and the PRC Special Pairs from the Crystal Structures of *R.v.*[1g−i] and *R.s.*[1f,h,i]

	2	**3**	**4**	**10**	**13**	**14**	*R.v.* SP	*R.s.* SP
Ct−Ct dist (Å)	5.15	4.66	5.39	4.96	5.36	5.35	7.37	7.64
M−M dist (Å)	5.11	4.63	5.38		5.36	5.33	7.58	7.73
MPS (Å)	3.61(3)	3.37(6)	3.6(3)	3.5(1)	3.5(2)	3.5(2)	3.3	3.8
interplanar angle (deg)	5.3	0.1	8.6	4.6	6.6	6.7	11.1	9.4
slip angle (deg)	46.8(4)	43.95(5)	49(4)	49(4)	50(4)	50(4)	65.7(3)	59(2)
lateral shift (Å)	3.75	3.23	4.07	3.74	4.11	4.09	6.72	6.59

Table 3. Crystallographically Derived Interdimer Geometrical Features for **2**−**4**, **10**, **13**, and **14**[a]

	compound											
	2		**3**		**4**		**10**		**13**		**14**	
macrocyclic core substituents	$Ni^{II}(1)-Ni^{II}(1)$	$Ni^{II}(2)-Ni^{II}(2)$	$Cu^{II}(1)-Cu^{II}(1)$	$Cu^{II}(2)-Cu^{II}(2)$	$Co^{II}(1)-Co^{II}(1)$	$Co^{II}(2)-Co^{II}(2)$	$Cu^{II}-Cu^{II}$	H_2-H_2	$Zn^{II}-Zn^{II}$	$Ni^{II}-Ni^{II}$	$Cu^{II}-Cu^{II}$	$Ni^{II}-Ni^{II}$
Ct−Ct dist (Å)	5.43	6.18	4.91		5.14	5.28	4.98		4.97	5.61	4.97	5.62
M−M dist (Å)	5.46	6.22	4.91		5.14	5.29	4.98		4.95	5.64	4.98	5.65
MPS (Å)	3.79	3.95	3.54		3.48	3.74	3.54		3.40	3.86	3.43	3.86
interplanar angle (deg)	0	0	0		0	0	0		0	0	0	0
slip angle (deg)	46.5	50.4	44.9		47.6	45.8	45.6		47.6	47.2	46.9	47.3
lateral shift (Å)	3.94	4.76	3.47		3.79	3.78	3.56		3.67	4.11	3.63	4.13

[a] Macrocycles are identified by their central metal ions (or hydrogen in the case of 10).

Table 4. Selected Bond Lengths (Å) for **4**, **10**, **13**, and **14**

4		**10**		**13**		**14**	
Co(1)−N(1)	1.959(4)	Cu(1)−N(1)	1.994(2)	Zn(1)−N(1)	2.034(3)	Cu−N(1)	1.994(2)
Co(1)−N(2)	1.992(4)	Cu(1)−N(2)	2.002(2)	Zn(1)−N(2)	2.041(3)	Cu−N(2)	2.005(3)
Co(1)−N(3)	1.964(4)	Cu(1)−N(3)	1.994(2)	Zn(1)−N(3)	2.051(3)	Cu−N(3)	2.000(2)
Co(1)−N(4)	1.972(5)	Cu(1)−N(4)	2.013(2)	Zn(1)−N(4)	2.057(4)	Cu−N(4)	2.010(3)
Co(2)−N(5)	1.962(4)	Cu(2)−N(5)	2.045(4)	Ni(1)−N(5)	1.942(3)	Ni−N(5)	1.936(2)
Co(2)−N(6)	1.936(5)	Cu(2)−N(6)	1.969(4)	Ni(1)−N(6)	1.929(3)	Ni−N(6)	1.923(3)
Co(2)−N(7)	1.963(4)	Cu(2)−N(7)	2.128(4)	Ni(1)−N(7)	1.926(3)	Ni−N(7)	1.944(3)
Co(2)−N(8)	1.941(4)	Cu(2)−N(8)	2.072(4)	Ni(1)−N(8)	1.911(3)	Ni−N(8)	1.932(3)
alkene bond	1.332(7)	alkene bond	1.336(4)	alkene bond	1.333(6)	alkene bond	1.337(4)

Table 5. Selected Bond Angles (deg) for **4**, **10**, **13**, and **14**

4		**10**		**13**		**14**	
N(1)−Co(1)-N(2)	88.6(2)	N(1)−Cu(1)-N(2)	88.73(9)	N(1)−Zn(1)-N(2)	178.74(13)	N(1)−Cu-N(2)	88.96(10)
N(1)−Co(1)-N(3)	179.7(2)	N(1)−Cu(1)-N(3)	179.80(9)	N(1)−Zn(1)-N(3)	91.03(13)	N(1)−Cu-N(3)	179.78(10)
N(1)−Co(1)-N(4)	91.9(2)	N(1)−Cu(1)-N(4)	90.82(9)	N(1)−Zn(1)-N(4)	89.13(13)	N(1)−Cu-N(4)	91.17(10)
N(3)−Co(1)-N(2)	91.4(2)	N(2)−Cu(1)-N(4)	179.37(9)	N(2)−Zn(1)-N(3)	88.57(13)	N(2)−Cu-N(4)	179.77(9)
N(3)−Co(1)-N(4)	88.2(2)	N(3)−Cu(1)-N(2)	91.41(9)	N(2)−Zn(1)-N(4)	91.24(13)	N(3)−Cu-N(2)	91.17(10)
N(4)−Co(1)-N(2)	179.4(2)	N(3)−Cu(1)-N(4)	89.05(9)	N(3)−Zn(1)-N(4)	178.78(13)	N(3)−Cu-N(4)	88.70(10)
N(5)−Co(2)-N(7)	178.3(2)	N(5)−Cu(2)-N(7)	176.1(2)	N(6)−Ni(1)-N(5)	89.49(14)	N(5)−Ni-N(7)	177.91(10)
N(6)−Co(2)-N(5)	88.9(2)	N(5)−Cu(2)-N(8)	93.25(14)	N(7)−Ni(1)-N(5)	177.84(14)	N(6)−Ni-N(5)	88.82(10)
N(6)−Co(2)-N(7)	90.5(2)	N(6)−Cu(2)-N(5)	89.04(14)	N(7)−Ni(1)-N(6)	90.91(14)	N(6)−Ni-N(7)	90.76(10)
N(6)−Co(2)-N(8)	180.0(2)	N(6)−Cu(2)-N(7)	93.2(2)	N(8)−Ni(1)-N(5)	90.69(14)	N(6)−Ni-N(8)	179.50(10)
N(8)−Co(2)-N(5)	91.1(2)	N(6)−Cu(2)-N(8)	177.1(2)	N(8)−Ni(1)-N(6)	179.52(14)	N(8)−Ni-N(5)	90.85(10)
N(8)−Co(2)-N(7)	89.5(2)	N(8)−Cu(2)-N(7)	84.45(14)	N(8)−Ni(1)-N(7)	88.90(14)	N(8)−Ni-N(7)	89.55(10)

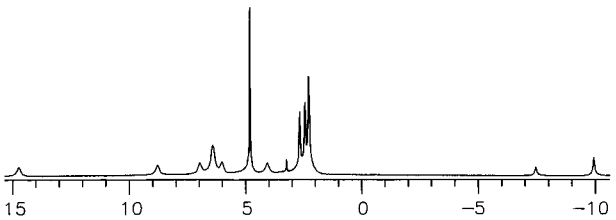

Figure 6. ^1H NMR spectrum of the di-Fe^{III} cyano analogue of **5** in CD_3OD.

X-ray Crystallographic Studies. Structure of *cis*-1,2-Bis-[cobalt(II) 5-(2,3,7,8,12,13,17,18-octaethylporphyrinyl)]ethene (4). The molecular structure of **4** is shown in Figure 5; selected geometrical measurements are given in Tables 2−5. Both central Co^{II} ions in the structure of **4** are tetracoordinate. The $Co^{II}(2)$ macrocycle exhibited a ruffled conformation[16] with a mean deviation of 0.219 Å for the macrocyclic atoms from the porphyrin mean plane[17] and an average Co(2)−N bond length of 1.95[1] Å (numbers given in brackets are average deviations from the mean). The $Co^{II}(1)$ macrocycle more closely approximated planarity, with a mean deviation of 0.072 Å for the macrocyclic atoms from the porphyrin mean plane. The average Co(1)−N bond length was 1.97[1] Å. The molecular structure of monomeric tetracoordinate $Co^{II}OEP$[18] is considerably less distorted than were both of the macrocycles of **4**. Extended aggregate stacks (similar to those illustrated in Figures 10 and 11) formed along the direction of the *a*-axis with $Co^{II}(1)$-bearing macrocycles facing $Co^{II}(1)$-bearing macrocycles and $Co^{II}(2)$-bearing macrocycles facing $Co^{II}(2)$-bearing macrocycles.

(16) Jentzen, W.; Simpson, M. C.; Hobbs, J. D.; Song, X.; Ema, T.; Nelson, N. Y.; Medforth, C. J.; Smith, K. M.; Veyrat, M.; Mazzanti, M.; Ramasseul, R.; Marchon, J.-C.; Takeuchi, T.; Goddard, W. A., III.; Shelnutt, J. A. *J. Am. Chem. Soc.* **1995**, *117*, 11085.
(17) Herein, "porphyrin mean plane" refers to the least-squares plane calculated for the 24 core carbon and nitrogen atoms.
(18) Scheidt, W. R.; Turowska-Tyrk, I. *Inorg. Chem.* **1994**, *33*, 1314.

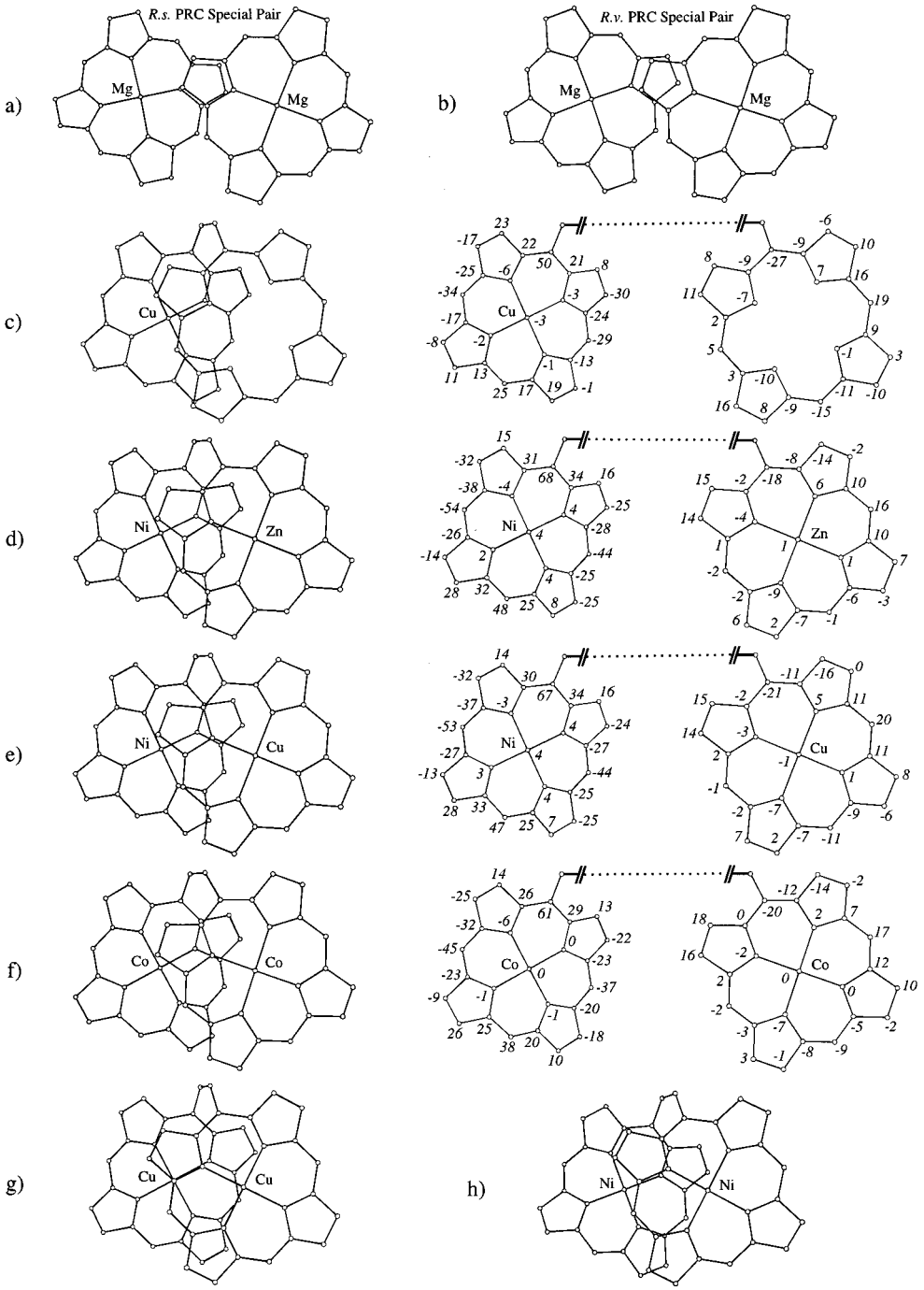

Figure 7. Top views of the molecular structures of the porphyrin macrocycles (without substituents) for (a) the *R.s.* PRC special pair[1f,h,i] (b) the *R.v.* PRC special pair[1g−i], (c) **10**, (d) **13**, (e) **14**, (f) **4**, (g) **3**,[4a,b] and (h) **2**.[4a,b] The structures are shown with the 4-N planes of the top macrocycles in the plane of the paper. At right for (c)−(f), the macrocycles are shown with the mean deviations (in Å × 100) of the macrocyclic atoms from their porphyrin mean planes.

Structure of *cis*-1-[Copper(II) 5-(2,3,7,8,12,13,17,18-octaethylporphyrinyl)]-2-[5-(2,3,7,8,12,13,17,18-octaethylporphyrinyl)]ethene (10). The molecular structure of **10** is shown in Figure 1; selected geometrical measurements are given in Tables 2−5. The Cu^{II} macrocycle exhibited a ruffled conformation with a mean deviation of 0.175 Å for the macrocyclic atoms from the porphyrin mean plane. The average Cu−N bond length was 2.001[7] Å. The shape of the Cu^{II} macrocycle, while being considerably different from that of monomeric Cu^{II}OEP[19] (which is planar) and most other Cu^{II} porphyrins, was, however, quite similar to one of the macrocycles in the previously reported **3**.[4a,b] The free-base macrocycle exhibited a wave conformation[16] and had a mean deviation of 0.096 Å for the macrocyclic atoms from the porphyrin mean plane.

Structure of *cis*-1-[Nickel(II) 5-(2,3,7,8,12,13,17,18-octaethylporphyrinyl)]-2-[zinc(II) 5-(2,3,7,8,12,13,17,18-octaethylporphyrinyl)]ethene (13). The molecular structure of **13** is shown in Figure 2; selected geometrical measurements are given in Tables 2−5. The Ni^{II} macrocycle demonstrated a ruffled conformation with a mean deviation of 0.262 Å for the macrocyclic atoms from the porphyrin mean plane. The average Ni−N bond length was 1.927[8] Å. The Ni^{II} macrocycle was

(19) Pak, R.; Scheidt, W. R. *Acta Crystallogr., Sect. C* **1991**, *47*, 431.

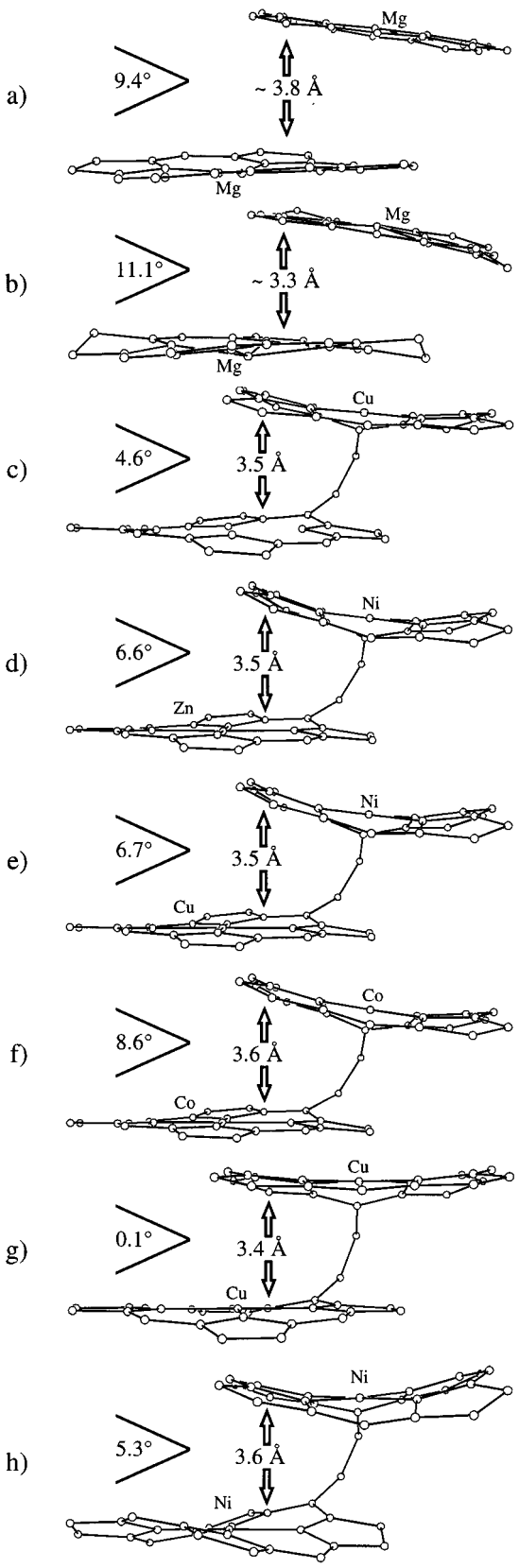

Figure 8. Side views of the molecular structures of the porphyrin macrocycles (without substituents) for (a) the special pair from the *R.s.* PRC[1f,h,i], (b) the special pair from the *R.v.* PRC[1g−i], (c) **10**, (d) **13**, (e) **14**, (f) **4**, (g) **3**,[4a,b] and (h) **2**.[4a,b] Structures are shown with the 4-N planes of the bottom macrocycles perpendicular to the plane of the paper. The inset on each figure is the mean plane separation (in Å) and the interplanar angle (in deg).

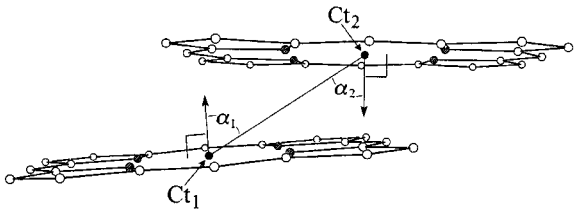

Figure 9. Illustration of the method by which the selected crystallographically derived geometrical features were measured. Macrocyclic centers (Ct) were calculated as the centers of the 4-N planes for each macrocycle. The interplanar angles were measured as the angle between the two macrocyclic 24-atom least-squares planes. Dimeric-OEP plane separations were measured as the perpendicular distance from one macrocycle's 24 atom least-squares plane to the center of the other macrocycle; reported dimeric-OEP mean plane separations (MPS) were the average of the two plane separations. PRC mean plane separations were measured as the average distance between the planes of the overlapping pyrroles. The slip angles (α) were calculated as the average angle between the vector joining the two macrocyclic centers and the unit vectors normal to the two macrocyclic 24 atoms least-squares planes ($\alpha = \alpha_1 + \alpha_2/2$). Lateral shift was defined as [sin(α) × (Ct−Ct distance)].[3c]

similar to the ruffled tetragonal form of $Ni^{II}OEP$[20] as well as many other Ni^{II} porphyrins among which ruffled conformations are a common moiety due to the relatively short nickel−nitrogen bond lengths. The Zn^{II} macrocycle exhibited a wave conformation, similar to many other tetracoordinate Zn^{II} porphyrins observed in the literature,[21a,b] and had a mean deviation of 0.073 Å for the macrocyclic atoms from the porphyrin mean plane. The Zn atom was tetracoordinate with an average Zn−N bond length of 2.046[8] Å. The positioning of the Zn atom was characteristic of tetracoordinate Zn porphyrins in that it was positioned in the porphyrin plane;[21a,b] in contrast to this are pentacoordinate Zn^{II} porphyrins which generally feature displacement of the central metal ion away from the porphyrin mean plane.[21c,d] Extended aggregate stacks formed along the direction of the *a*-axis with Ni^{II}-bearing macrocycles facing Ni^{II}-bearing macrocycles and Zn^{II}-bearing macrocycles facing Zn^{II}-bearing macrocycles (Figures 10 and 11).

Structure of *cis*-1-[Nickel(II) 5-(2,3,7,8,12,13,17,18-octaethylporphyrinyl)]-2-[copper(II) 5-(2,3,7,8,12,13,17,18-octaethylporphyrinyl)]ethene (14). The molecular structure of **14** is shown in Figure 3; selected geometrical measurements are given in Tables 2−5. The Ni^{II} macrocycle exhibited a ruffled conformation (similar to the Ni^{II}-bearing macrocycle in the structure of **13**) with a mean deviation of 0.259 Å for the macrocyclic atoms from the porphyrin mean plane. The average Ni−N bond length was 1.934[6] Å. The Cu^{II} macrocycle exhibited a wave conformation (similar to the Zn^{II}-bearing macrocycle in the structure of **13**) and demonstrated a mean deviation of 0.078 Å for the macrocyclic atoms from the porphyrin mean plane. The average Cu−N bond length was 2.002[5] Å. The Cu^{II} macrocycle was somewhat different from that of monomeric $Cu^{II}OEP$,[19] which is nearly planar. Extended aggregate stacks (similar to those illustrated in Figures 10 and 11) formed along the direction of the *a*-axis with Ni^{II}-bearing macrocycles facing Ni^{II}-bearing macrocycles and Cu^{II}-bearing macrocycles facing Cu^{II}-bearing macrocycles.

(20) Meyer, E. F., Jr., *Acta Crystallogr., Sect. B* **1972**, *28*, 2162.
(21) (a) Scheidt, W. R.; Mondal, J. U.; Eigenbrot, C. W.; Adler, A. D.; Radonovich, L. J.; Hoard, J. L. *Inorg. Chem.* **1986**, *25*, 795. (b) Byrn, M. P.; Curtis, C. J.; Hsiou, Y.; Khan, S. I.; Sawin, P. A.; Tendick, S. K.; Terzis, A.; Strouse, C. E. *J. Am. Chem. Soc.* **1993**, *115*, 9480. (c) Barkigia, K. M.; Berber, M. D.; Fajer, J.; Medforth, C. J.; Renner, M. W.; Smith, K. M. *J. Am. Chem. Soc.* **1990**, *112*, 8851. (d) Brennan, T. D.; Scheidt, W. R. *Acta Crystallogr., Sect. C* **1988**, *44*, 478.

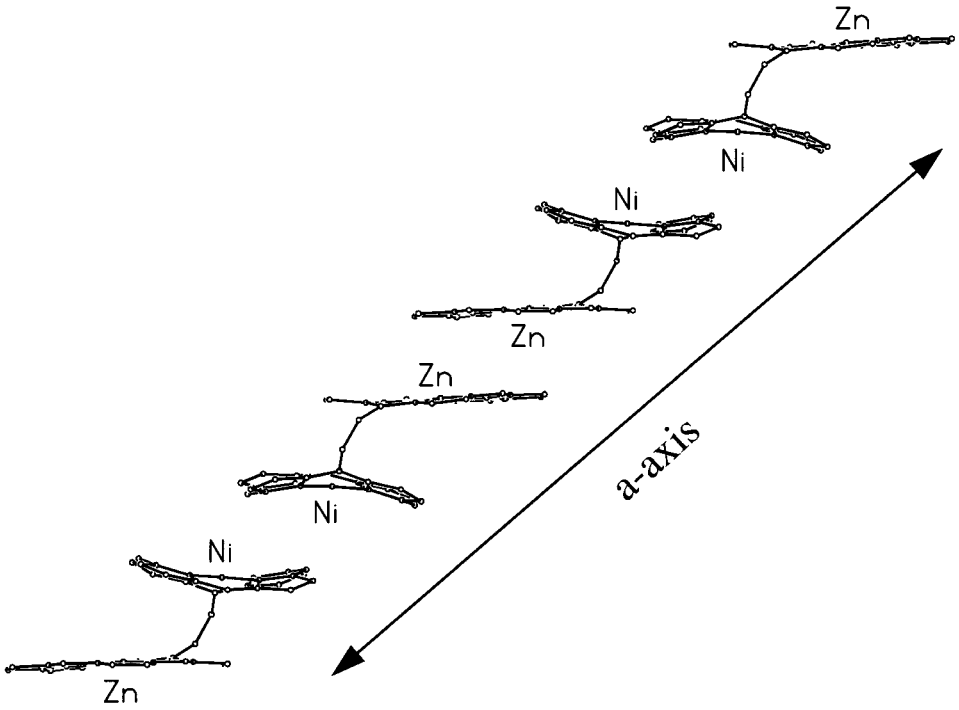

Figure 10. Side view of the crystal packing of bisporphyrin **13**. Ethyl side chains have been omitted for clarity.

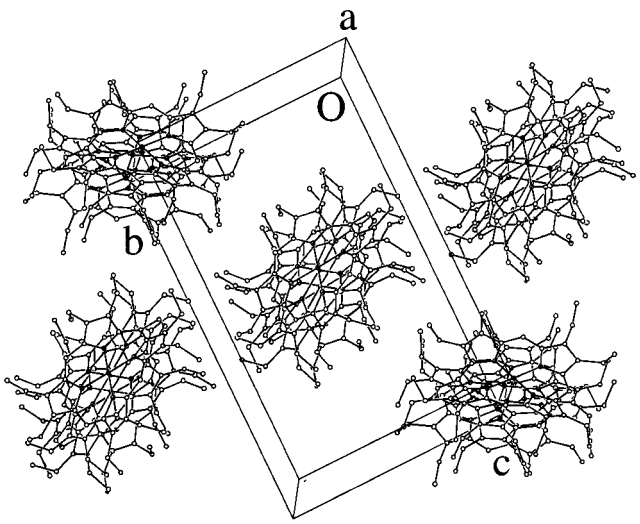

Figure 11. View of the crystal packing of bisporphyrin **13** illustrating the pillared formations of dimer stacks along the direction of the *a*-axis.

Structure of *trans*-1-[Chloromanganese(III) 5-(2,3,7,8,12,-13,17,18-octaethylporphyrinyl)]-2-[copper(II) 5-(2,3,7,8,12,-13,17,18-octaethylporphyrinyl)]ethene (15). The X-ray crystal structure of **15** was disordered such that it was not possible to obtain a satisfactorily refined crystal structure. The data obtained did, however, clearly demonstrate the trans geometry of the linking ethene bond.

After the publication of the PRC crystal structures a number of dimeric tetrapyrroles were prepared as models of the special pair.[2−4,10] The present work is a continuation of those studies which have attempted to attain closer approximations of the situation encountered in vivo. Figures 7 and 8 compare the structures of the bisporphyrins **2**−**4**, **10**, **13**, and **14** with the crystallographically determined structures of the *R.s.*[1f,h,i] and *R.v.*[1g,h,i] PRC special pairs. Selected geometrical features for these comparisons are given in Table 2 (the calculations employed in the measurement of these geometrical features are illustrated in Figure 9). In the *R.s.* special pair we observed an interplanar separation of ∼3.8 Å and an interplanar angle of 9.4°, while in the *R.v.* special pair we observed an interplanar separation of ∼3.3 Å and an interplanar angle of 11.1°. Our systems are a good match regarding these features and display interplanar separations ranging from 3.4 to 3.6 Å and interplanar angles ranging from 0.1 to 8.6°. An additional important geometrical feature regards the degree of intramolecular macrocyclic π overlap. In both of the special pairs the overlap was restricted to one pyrrolic subunit of each bacteriochlorophyll monomer and lateral shifts of 6.59 Å (for *R.s.*) and 6.72 Å (for *R.v.*) were observed. A feature common to the cofacial 1,2-bis[5-(2,3,7,8,12,13,17,18-octaethylporphyrinyl)]ethenes is a degree of macrocyclic overlap equal to approximately half of the porphyrin macrocycle (Figure 7). We have reduced the degree of macrocyclic overlap (illustrated in Figure 7 and evidenced in the increased lateral shifts given in Table 2) in comparison to our previous model systems[4a,b] (**2** and **3**), and presently we observe a 3.74−4.11 Å range of intramolecular lateral shifts (**4**, **10**, **13**, **14**). It should be noted that in systems of this type $\pi-\pi$ interactions demonstrate a tendency to pull the macrocycles into a degree of overlap which is greater than has been observed in the special pair. Future efforts to refine this type of special pair model should seek to further increase the lateral shifts in order to more closely model the special pair.

A feature common to the 1,2-bis[5-(2,3,7,8,12,13,17,18-octaethylporphyrinyl)]-ethenes is that one macrocycle generally adopted a nonplanar ruffled conformation while the other macrocycle more closely approximated planarity (as evidenced by the out-of-plane displacements illustrated in Figure 7). The one exception to this was **2** in which both macrocycles exhibited ruffled conformations; however, even in the structure of **2**, one macrocycle was significantly more nonplanar than the other.[4a,b] Another trend observed for this series was that the bridging meso carbons always deviated more from the porphyrin mean planes than did the nonbridging meso carbons due to the strain inherent in the overall geometry of these systems.

Compounds **2**, **4**, **13**, and **14** were very similar in their crystal packing; all were monoclinic, space group $P2_1/c$, with nearly

identical cell dimensions. While there do exist a number of structural differences between the individual molecules, their crystal packing was generally isostructural. Each formed extended aggregate stacks along the direction of the *a*-axis with inversion centers between adjacent stacked molecules (Figures 10 and 11). Compounds **3** and **10** were monoclinic, space group $P2_1/n$, and had nearly identical cell dimensions and internal symmetry. The crystal packing for **3** and **10** showed that dimer pairs formed with inversion centers between them. However, unlike the cell packing observed in **2**, **4**, **13**, and **14**, stacking was not in an extended fashion but rather it was limited to two dimers per stack. In the case of **3**, paired dimer stacks terminated with $Cu^{II}(2)$ macrocycles [$Cu^{II}(1)$ and $Cu^{II}(2)$ bearing macrocycles were structurally distinct], and in the case of **10**, paired dimer stacks terminated with free-base macrocycles. Among the cofacial dimers in this series (**2**−**4**, **10**, **13**, **14**) intermolecular cofacial arrangements were always separated by inversion centers. A ramification of the inversion centers was evidenced in the intermolecular interplanar angles of 0° as shown in Table 3.

Of further interest are the intramolecular interplanar angles between macrocycles. In the absence of steric and/or electronic effects we would expect the interplanar angles to be approximately 60° due to the linking alkenic bond. However, the range of intramolecular interplanar angles observed for this class of compounds was 0.1−8.6° indicating that intramolecular $\pi-\pi$ interactions play an important role. Scheidt and Lee proposed a semiquantitative scheme based upon lateral shifts for classifying tightly held porphyrin dimers in the solid state (these dimers were not necessarily covalently bound but rather were defined by the spatial orientations of adjacent porphyrin monomers within the crystalline lattice). All appropriate known porphyrin dimer crystal structures were evaluated, and their lateral shifts and mean plane separations were compared. The results of the study revealed three clusters of compounds, those with lateral shifts of ∼1.5 Å (deemed group S, small lateral shifts), those with lateral shifts of ∼ 3.5 Å (deemed group I, moderate lateral shifts), and those with lateral shifts ranging from 4 to 8 Å (deemed group W). Sheidt and Lee believed that compounds in groups S and I represented real $\pi-\pi$ interactions and that their 3-dimensional structures were not determined merely by efficient crystalline packing. However, they stated that the likelihood of $\pi-\pi$ interactions among members of Group W was less certain, and that solid state geometric features of these compounds were likely to be determined, either completely or in part, by efficient crystalline packing.[22] Among the cofacial 1,2-bis[5-(2,3,7,8,12,13,17,18-octaethylporphyrinyl)]ethenes, we observed intramolecular mean plane separations ranging from 3.4 to 3.6 Å and lateral shifts ranging from 3.2 to 4.1 Å (Table 2 and Figure 8). Intermolecular interactions were also apparent for the entire series with mean plane separations ranging from 3.40 to 3.95 Å and lateral shifts ranging from 3.47 to 4.76 Å (Table 3).

Conclusions

A novel series of monometallic, heterobimetallic and bimetallic bisporphyrins have been synthesized, demonstrating the stability of this readily accessible cis-dimeric framework (**1**). Two heterobimetallic cofacial bisporphyrins (**13** and **14**) were synthesized with ease by initially forming monometalated species (**9** and **10**), with subsequent insertion of a second metal ion. The initial (mono)metalations were shown to be slow under dilute conditions in CH_2Cl_2/MeOH at reflux; however, under dilute conditions in hot DMF the insertion rate was sufficiently fast to enable isolation of the monometalated cofacial isomers as the major product. Unfortunately, the cofacial isomer (**21**) of bisporphyrin **15** could not be prepared because the elevated temperatures used for manganese insertion into porphyrins are too vigorous to maintain the cis-configuration of the bisporphyrin. The di-Co^{II} (**4**) and di-Fe^{III} (**5**) cofacial bisporphyrins were also obtained in good yield. The cofacial bisporphyrins **4**, **10**, **13**, and **14** were characterized using X-ray crystallography and evaluated for structural similarity to the PRC "special pair". Comparison of several geometrical features demonstrated a number of similarities. These bisporphyrins more closely resembled the special pair than did our previous model systems (**2**, **3**) in that they displayed larger lateral shifts between their macrocycles. Electrochemical, photochemical excited-state, and ligand binding studies of the metal complexes described above are in progress.

Acknowledgment. This work was supported by grants from the National Institutes of Health (HL 22252) and the National Science Foundation (CHE-96-23117).

Supporting Information Available: X-ray crystallographic files for **4**, **10**, **13**, and **14**, in CIF format. Thermal ellipsoid plots (4 pages). Ordering and access information is given on any current masthead page.

IC970774P

(22) Scheidt, W. R.; Lee, Y. J. *Struct. Bonding (Berlin)* **1987**, *64*, 30−31.